Regulation of Dopamine D1 Receptor Signaling at the Golgi Apparatus by a Low Affinity Dopamine Transporter

Natasha M. Puri [1 #], Giovanna R. Romano[1,2 #], Quynh N. Mai[3] and Roshanak Irannejad[1,3*]
[1]Department of Biochemistry & Biophysics, University of California, San Francisco, USA,
[2]Biochemistry Department, Weill Cornell Medicine, USA, Cardiovascular Research Institute, University of California, San Francisco, USA
[#]These authors contributed equally
*Corresponding author

Abstract
G protein-coupled receptors (GPCRs) are the largest family of membrane receptors expressed in humans. It has been traditionally thought that GPCRs can only signal on the plasma membrane, where receptors are activated upon binding of external cues. However, recent work has demonstrated that, in several cases, subcellularly-localized GPCRs are also activated upon the presence of external cues resulting in downstream signaling pathways. Whether subcellular activation of GPCRs is limited to subsets of GPCRs or is a general aspect of GPCR signaling is not known. Additionally, establishing GPCR signaling from subcellular compartments is the first step in unraveling the physiological consequences of compartmentalized signaling for each GPCR family member. Here, using novel nanobody-based biosensors, we demonstrate that dopamine D1 receptor (D1DR), the primary mediator of dopaminergic signaling in the brain and kidney, is activated at both the plasma membrane and the Golgi apparatus upon the presence of its ligand. Interestingly, we found that activation of the Golgi pools of D1DRs is dependent on Organic Cation Transporter 2 (OCT2), a low affinity dopamine transporter, providing an explanation for how dopamine, a membrane impermeant ligand, accesses subcellular pools of D1DR. We also show that Golgi-localized D1DRs regulate local cAMP production and mediate protein kinase A activation at the Golgi membranes. Together, our data suggest that spatially compartmentalized signaling hubs are previously unappreciated regulatory aspects of D1DR signaling. Our data also provide further evidence for the role of transporters in regulating subcellular GPCR activity.

Introduction
Dopamine (DA) is a major hormone and neurotransmitter that is produced locally in the central nervous system (CNS) and the kidney. DA regulates important physiological responses ranging from reward-motivated behavior and motor control in the CNS as well as sodium secretion in the kidney (1-3). All of cellular actions of DA are mediate by Dopamine receptors, a class of GPCR. There are five subtypes of Dopamine receptors, D1, D2, D3, D4 and D5 that are classified as D1-class receptors (D1 and D5) or D2-class receptors (D2, D3 and D4) (4, 5). The D1-class (D1 and D5 receptors) are primarily coupled to Gαs/olf proteins and stimulate the activity of adenylate cyclase, AC, leading to the production of the second messenger cyclic AMP, cAMP. In contrast, the D2 class (D2S, D2L, D3 and D4 receptors) are associated with Gαi/o proteins and inhibit cAMP production (6). D1 Dopamine Receptors (D1DR) are highly expressed in the CNS and the kidney where they underlie major physiological functions of dopamine in these organ systems.

Impermeable agonists such as DA have been thought for a long time to activate D1DR only at the plasma membrane. Like many GPCRs, receptor removal from the cell surface by endocytosis, has been described as a mechanism that attenuates cellular signaling (7-9). However, evidence from the past decade suggests that for some GPCRs endocytosis might in fact activate a second phase of acute or prolonged Gαs-mediated cAMP response from the endosomes (10-20). Recent studies further support this notion by providing evidence that cAMP generation by activated receptors at the endosome are necessary in regulating transcriptional responses that are distinct from those elicited by activation of the plasma membrane receptor pool (21-25).

Most of the receptors that have been shown to exhibit a second phase of signaling from internal compartments are primarily coupled to Gαs protein. cAMP diffusion is within the nanometer scale around phosphodiesterase at physiological conditions(26, 27). Given this narrow range of diffusion, it has been difficult to explain how receptor activation solely on the plasma membrane results in the activation of downstream effectors at distant subcellular locations such as the endoplasmic reticulum, Golgi and the nucleus (27-29). As one explanation for this observation, we recently showed that activation of the Golgi-localized beta1 adrenergic receptors (β1AR) causes local production of cAMP by Golgi membrane localized activated Gαs protein. Supporting the notion that cAMP production from distinct subcellular locations regulates distinct cellular outcomes, we also found that the cAMP response elicited by the Golgi-β1AR, but not the plasma membrane pool, leads to the activation of a PLCe-mediated hypertrophic response. This PLCe complex is localized at the perinuclear region of the cardiomyocytes (30, 31).

Considering the high degree of membrane compartmentation of neurons and proximal tubules of the kidney, the two main cells types that express D1DRs, we wondered whether D1DR signaling is also compartmentalized. Here, using a conformational sensitive nanobody that recognizes activated D1DR, we show that the pool of D1DR that is localized to the Golgi membrane is activated upon stimulation with extracellular DA. Furthermore, we demonstrate that a low affinity dopamine transporter, an Organic Cation Transporter (OCT2), facilitates the transport of DA to the Golgi-localized D1DR and regulates its local activity at the Golgi. We further show that OCT2 is mainly expressed in the kidney cells where D1DRs are endogenously expressed. Our findings thus identify a specific role for a monoamine transporter in regulating a specific pool of the D1DRs and their function in a physiologically relevant model of dopaminergic signaling.

Results

Nanobody-based conformational sensitive biosensors detect active D1DR and Gs protein at subcellular membranes. We have previously shown that nanobody 80 (Nb80), originally developed to stabilize an active conformation of beta 2 adrenergic receptor (β2AR) for crystallography purposes(32), can be repurposed as a conformational biosensor to detect activated β2AR and β1AR in living cells(14, 30). Through directed evolution on Nb80, a high-affinity nanobody (Nb6B9) was generated that stabilizes the active conformation of epinephrine bound β2AR (33). Given that β2AR/Nb6B9 binding sites are highly conserved among other aminergic receptors such as β1AR and D1DR (Supplementary Figure 1)(32), we reasoned that this nanobody could also be used as a

conformational sensitive biosensor to detect activated D1DR in real time and in living cells (Figure 1a). In HeLa cells expressing Snap-tagged D1DR, Nb6B9 fused to GFP (Nb6B9-GFP) was diffuse throughout the cytoplasm (Figure 1b, 0min). Upon stimulation of D1DR expressing HeLa cells with 10μM DA, Nb6B9-GFP was rapidly recruited first to the plasma membrane and shortly after to another subcellular location, the Golgi apparatus (Figure 1b, 2min, Supplementary Movie 1). This data suggests that D1DR Golgi pool is activated in response to extracellular DA addition. Interestingly, stimulation of 10μM DA in HEK293 cells expressing D1DR resulted in the recruitment of NB6B9-GFP only at the plasma membrane (Figure 1b, lower panel, 2min, Supplementary Movie 2). However, in both cell types, SKF81297, a selective membrane permeant D1DR agonist, activated both receptor pools (Supplementary Figure 2 and Supplementary movie 3 and 4). In addition to the Golgi recruitment and consistent with a previous report (13), Nb6B9 was also found to colocalize with D1DR at the endosomes, at a later time after agonist addition, indicating an active pool of D1DR at endosomes (Supplementary Movie 2). We further used mini-Gs protein, a biosensor for Gs-coupled GPCR(34), to show that the active pool of D1DR at the plasma membrane, endosomes, and the Golgi can also be detected by mini-Gs recruitments to these locations (Supplementary Figure 3).

To investigate whether activated D1DR can couple to G protein and elicit a G-protein mediated response at the Golgi, we took advantage of another nanobody-based biosensor, Nb37-GFP. We previously used Nb37-GFP to detect transiently active β1AR/Gs and β2AR/Gs complexes at the Golgi and endosomes, respectively (14, 30). Similar to what we previously observed with β1AR, Nb37 was recruited to the plasma membrane and the Golgi upon stimulation with DA, suggesting that D1DR Golgi pool is able to couple to G protein and activate it (Supplementary Figure 4b and c). Together, these findings suggest a distinct spatiotemporal regulation of D1DR signaling at the plasma membrane and the Golgi membranes.

OCT2 facilitates the transport of Dopamine to the Golgi-localized D1DR.

These observations raised a key question of how DA, a hydrophilic/membrane impermeant monoamine, can access the Golgi pool of D1DR. The first clues came from the observation that DA can activate Golgi-D1DR in HeLa cells but not HEK293 cells (Figure 1b, Supplementary Movie 1 and 2) whereas, SKF81297, a hydrophobic/membrane permeant agonist can activate the Golgi pool of D1DR in both cell types (Supplementary Figure 2, Supplementary Movie 3 and 4). These differential effects of DA and SKF81297 are not based on their differential potency for activating D1DR, as they have comparative EC50 values in inducing cAMP responses (Figure 2a). Moreover, D1DR activation at the Golgi was not dependent on receptor internalization, as inhibiting endocytosis, by blocking dynamin, did not block D1DR activation at the Golgi (Supplementary Figure 4a and c). We previously found that a membrane transporter, Organic Cation Transporters 3 (OCT3), facilitates epinephrine transport resulting in activation of the Golgi-localized β1AR. OCT3 is a member of the solute carrier (SLC) family 22, electrogenic and bidirectional catecholamine transporters that are localized on the plasma membrane and intracellular compartments (30). Therefore, we hypothesized that another OCT family transporter can similarly function in DA transport to allow for the activation of Golgi-localized D1DR pools.

There are three main OCTs that have largely overlapping distribution but distinctly different substrates. OCT3 facilitates the transport of epinephrine and norepinephrine (21103969). DA, has been identified as key endogenous substrate for another member of the SLC22A family, OCT2 (SLC22A2)(35-38). We thus asked whether OCT2 has a role in transporting DA to the Golgi membranes. OCT2 showed significant protein expression in HeLa cells as measured by western blotting, whereas no significant expression was detected in HEK293 cells (Figure 2b). To test the role of OCT2 in DA transport, we then overexpressed OCT2-mApple in HEK293 cells and used Nb6B9-GFP to assess D1DR activation in live cells. By overexpressing OCT2-mApple in HEK293 cells, we found that Nb6B9-GFP could now be recruited to activated D1DR at the Golgi. (Figure 2c and d, Supplementary Movie 5). These results suggest that OCT2 can facilitate the transport of DA to the Golgi lumen where it can then lead to the activation of D1DR at the Golgi membranes. To investigate the role of OCT2 in D1DR signaling in a more physiologically relevant cell type, we used MDCKs, a kidney derived cell type. We found that D1DRs and OCT2 can be detected at both the plasma membrane and the Golgi pools (Supplementary Figure 5).

Golgi and plasma membrane-localized D1DR both contribute to the cAMP response

Our data suggested that plasma membrane and the Golgi pools of D1DR can both couple to the Gs protein. In addition to its presence at the plasma membrane, adenylyl cyclase has been reported to localize at the Golgi/perinuclear membranes (39, 40). We therefore asked whether D1DR/Gs complexes at both the plasma membrane and the Golgi activate Gs-mediated cAMP responses. To address this question, we utilized a rapamycin dimerization system composed of FK506-binding protein (FKBP) and FKBP-rapamycin binding domain of FRAP (FRB), to rapidly induce recruitment of Nb6B9 to specific membrane compartments. This makes it possible to specifically block D1DR/Gs coupling at each distinctly localized pool. We have previously shown that βARs nanobody, Nb80, which binds to the same region as G protein (32, 41), blocks either the plasma membrane or the Golgi-β1AR mediated cAMP responses when it is recruited locally to these compartments at high concentrations(30). This inhibition is likely due to steric occlusion of Gαs protein. Using HEK293 cells expressing either FKBP at the plasma membrane or the Golgi with FRB fused to Nb6B9 (FRB-Nb6B9), we demonstrated that treatment with rapamycin specifically targets Nb6B9 to either membranes (Figure 3 a-c). Upon stimulation with membrane permeant agonist SKF81297, Nb6B9 targeted to the plasma membrane disrupts plasma membrane-D1DR /G proteins coupling, while Golgi-D1DR is still able to elicit a cAMP response (Figure 3d). In turn, treatment with rapamycin in cells expressing Golgi-targeted FKBP and FRB-Nb6B9 and subsequent stimulation with SKF81297 resulted in only activation of the plasma membrane-D1DR pool (Figure 3e). Importantly, rapamycin treatment alone had no effect on the overall cAMP production elicited by Forskolin, a direct activator of adenylyl cyclase (Figure 3f). These data indicate that Golgi-localized D1DR is able to activate cAMP response.

Local activation of PKA at the Golgi depends on selective activation of Golgi-localized D1DR

A key downstream effector sensed by cAMP, is protein kinase A (PKA). PKA is a holoenzyme, consisting of two catalytic and two regulatory subunits (Figure 4a). There are two PKA types (type I and II) that are anchored to distinct subcellular locations through interactions with distinct A kinase anchoring proteins (42). PKA type II has been shown to localize to the Golgi membranes (43). Binding of cAMP to PKA regulatory subunit, induces dissociation and activation of PKA catalytic subunit (Figure 4a) (44, 45). To test whether cAMP generation by Golgi-localized D1DR/Gs complex results in the activation of PKA at the Golgi, we utilized a previously described HEK293T knock-in cell line expressing a split fluorescent protein, labeling native PKA catalytic subunit gene with GFP (PKAcat-GFP) (28851864). Stimulation of HEK293T PKAcat-GFP knock in cells lines expressing D1DR with 10nM SKF81297, a concentration that activates both pool of D1DR (Supplementary Figure 3), resulted in rapid dissociation of PKAcat-GFP from the perinuclear/Golgi membranes (Figure 4b top panel). Quantification of this data shows that stimulation with SKF81297 results in sustained activation of PKA at the Golgi (Figure 4c, Supplementary Figure 6). We then asked whether PKAcat dissociation is mediated by the activation of D1DR Golgi pool. Given that HEK293T cells do not express the OCT2 transporter (Figure 2b) and thus DA cannot be transported to the Golgi membranes, we used DA to specifically activate the plasma membrane pool of D1DR. Importantly, stimulation of HEK293T PKAcat-GFP knock-in cells with 10nM DA, a concentration with similar potency as SKF81297 (Figure 2a), did not cause PKAcat dissociation from the Golgi (Figure 4 b, lower panel, and c). Together, these data indicate that activation of the D1DR at the Golgi, but not the plasma membrane, results in PKA activation at the Golgi.

Discussion

Our findings demonstrate for the first time that dopaminergic receptors can signal from the Golgi apparatus. We present evidence that dopamine, a hydrophilic catecholamine, can be transported to the Golgi membrane to reach the Golgi-localized D1DRs. This transport is facilitated by a low affinity dopamine transporter, OCT2. The Golgi-D1DR comprises a functional signaling pool as it can activate Gαs and stimulate cAMP production. Moreover, we have introduced a new approach to selectively interrogate compartmentalized D1DR signaling by inhibiting Gαs coupling, using a nanobody-based chemical recruitment approach.

The present study also demonstrates the important role of local generation of cAMP by GPCRs, in controlling local PKA activation at specific subcellular compartments. It is well established that signaling specificity mediated by cAMP depends on the function of compartment specific phosphodiesterases, enzymes that degrades cAMP limiting its diffusion (3, 46-50). Recent measurements of cAMP mobility suggest a nanometer scale diffusion domain (26, 27). Consistent with this, our data provide evidence that PKA activation at a compartment requires GPCR activation locally at that compartment.

We found that OCT2 can facilitate the transport of DA to the Golgi resulting in activation of the Golgi-D1DR pools. As we found in the case of MDCK cells, published evidence suggests that OCT2 is expressed in a number of tissues and cells types that also express D1DRs(36, 51, 52). Interestingly, however, there are D1DR expressing cell types that do not appear to express OCT2. For example, within the brain OCT2 is mainly expressed in

the striatum but not in the cortex or substantia nigra, regions where D1DR has known functions (36). Therefore, we speculate that expression pattern of OCT2 may be a determinant on which cell types and tissues exhibit activation of Golgi-pool of D1DRs.

Figure legends:

Figure 1. Conformational biosensor detects activated D1DR at the plasma membrane and the Golgi upon Dopamine stimulation. a. Nb6B9 binds to the receptor exclusively in its active conformation. We fused Nb6B9 to GFP and used it as conformational biosensor for D1DR. **b.** Confocal images of representative D1DR-expressing HeLa (top panel) and HEK293 cells (lower panel) with Nb6B9-GFP and GalT-mRFP expression before and after 10µM dopamine addition. Stimulation with 10uM dopamine results in recruitment of Nb6B9 to active D1DR at plasma membrane and Golgi in HeLa (*n* = 15 cells, Pearson's coefficient = 0.63, respectively, 5 experiments); 10µM DA treatment only activates plasma membrane localized D1DR in HEK 293 cells (*n* = 17 cells, Pearson's coefficient = 0.15, 5 experiments). Right panels show merged images of Nb6BP and the Golgi marker. Arrows indicate active D1DR at plasma membrane; Arrowhead indicates active D1DR at Golgi membrane; Scale bar = 10µm **c.** Quantification of D1DR activity at Golgi in HeLa and HEK293 cells; Normalized fluorescence intensity of Nb6B9 at Golgi relative to D1DR at Golgi labeled with Snap-tagged.

Figure 2. OCT2 facilitated DA transport to the Golgi-Localized D1DR. a. Dose-response curve of forskolin-normalized D1DR-mediated cAMP response in HEK 293 cells treated with SKF81297 or dopamine; SKF and DA have similar potency and efficacy, thus differences in signaling at Golgi in HEK293 cells are not due to differences in drug potency or efficacy (mean ± s.e.m., *n* = 3 biological replicates). **b.** Detection of OCT2 expression by Western Blot. HeLa cells express OCT2, while HEK 293 cells do not. **c.** Representative HEK293 cell expressing Snap-D1DR, Nb6B9-GFP, and OCT2-mApple at indicated times after 10µM addition. Overexpression of OCT2 in HEK293 cells rescues Golgi-localized D1DR activation (*n* = 16 cells, Pearson's coefficient = 0.67, 6 experiments). Arrow indicates active D1DR at plasma membrane; Arrowhead indicates active D1DR at Golgi membrane; Scale bar = 10µm. **d.** Quantification of Nb6B9-GFP recruitment at Golgi in HEK293 cells with or without OCT2 overexpression; Normalized fluorescence intensity of Nb6B9-GFP relative to Snap D1DR at Golgi.

Figure 3. Both plasma membrane and Golgi-localized D1DR promote cAMP production. Model of blocking D1DR-Gs coupling at the plasma membrane (**a**) and Golgi membrane (**b**) after recruitment of mVenus-FRB-Nb6B9. FKBP was targeted to either the plasma membrane (**a**) or Golgi membrane (**b**), and its binding partner FRB-mVenus was fused to Nb6B9. Upon addition of rapalog (rapamycin analog), FKBP and FRB heterodimerize and sequester Nb6B9 to either membranes, disrupting G protein coupling to the receptor and thus blocking signaling from each respective location. **c.** Representative confocal images of HEK293 cells expressing either plasma membrane (PM) or Golgi targeted FKBP showing mVenus-FRB Nb6B9 localization at indicated times after rapalog addition. Representative cells confirm inducible sequestration of Nb6B9 to either PM or Golgi. Arrow indicates PM; Arrowhead indicates Golgi. **d.** Forskolin-normalized D1DR-mediated cAMP response with and without rapalog pretreatment (1µM,

15 min) and SKF81297 at indicated concentrations in HEK293 expressing PM-FKBP (mean ± s.e.m., *n* = 6 biological replicates, P values of 0.0021 and 0.0015 at 10^{-7} and 10^{-6}, respectively) **e.** Forskolin-normalized D1DR-mediated cAMP response with and without rapalog pretreatment (1µM, 15 min) and SKF81297 at indicated concentrations in HEK293 expressing Golgi-FKBP (mean ± s.e.m., *n* = 6 biological replicates, P values of <0.0001 at 10^{-7} and 10^{-6}). **f.** Effect of 1µM and 10µM rapalog on forskolin-mediated cAMP response (*n* = 3 biological replicates)

Figure 4. Golgi localized PKA is activated by D1DR at the Golgi. a. Model of PKA activation; cAMP binds PKA regulatory subunit (R), rendering PKA catalytic subunit (PKA-cat) dissociation. **b.** Confocal images of representative D1DR-expressing HEK293 cells with endogenous PKA-cat-GFP and GalT-mRFP expression at indicated times after 10nM SKF81927 (top panels; *n* = 11 cells, Pearson's coefficient 0.53, 3 biological replicates) or 10nM DA (lower panels, *n* = 12 cells, Pearson's coefficient = 0.64, 3 biological replicates). Arrowhead indicates PKAcat at Golgi membrane; Scale bar = 10µm. **c.** Normalized fluorescence intensity of PKAcat relative to Golgi-D1DR after treatment with 10nM DA or 10nM SKF81927.

Supplementary Figure 1. Motifs of nanobody binding are conserved between β2AR and D1 dopamine receptor (D1DR).

Supplementary Figure 2. Conformational biosensor detects activated D1DR at the plasma membrane and the Golgi upon SKF81297 stimulation. Representative Flag-D1DR-expressing HEK293 and HeLa cells with Nb6B9-GFP and GalT-mRFP localization at indicated times after 10uM SKF81297 addition. Stimulation with 10uM SKF81297 results in recruitment of Nb6B9 to active D1DR at plasma membrane and Golgi in both HEK 293 and HeLa cells. Scale bar = 10µm.

Supplementary Figure 3. MiniGαs protein biosensor detects active D1DR at the plasma membrane and the Golgi. Representative Snap-D1DR-expressing HeLa cell with miniGs-mVenus and GalT-mRFP localizations at indicated times after 10nM SKF81297 (top panels) and DA (lower panels) addition. Scale bar = 10µm.

Supplementary Figure 4. a. Representative HeLa cell expressing Snap-D1DR and Nb6B9-GFP. Cells were incubated with 30µM Dyngo-4a, a dynamin inhibitor that blocks endocytosis, stimulated with 10µM DA at indicated times. Golgi-localized D1DR is activated when endocytosis is blocked, suggesting that activation of the Golgi pool is not dependent on D1DR internalization. **b.** Representative HeLa cell expressing Snap-D1DR and Nb37-GFP at indicated times after 10µM DA addition. Nb37 binds to the GPCR-Gs protein complex in the nucleotide free state. Scale bar = 10µm. **c.** Quantification of Nb37-GFP and Nb6B9-GFP intensity at Golgi, normalized to Golgi-D1DR. Both nanobodies show similar kinetics of Golgi-localized D1DR activation after addition of 10µM DA.

Supplementary Figure 5. a. Endogenous localization of D1DR and **b.** OCT2 at the plasma membrane and the Golgi membranes**.** MDCK cells were labeled with D1DR and

OCT2 specific antibody and the Golgi antibody (GM130). Arrowheads indicate Golgi localizations. Arrows indicate plasma membrane localization.

Supplementary Figure 6. Kinetics of PKAcat-GFP dissociation from the Golgi membrane upon activation of the D1DR Golgi Pools.

Supplementary Movie 1. Confocal image series of D1DR expressing HeLa cells (Magenta), Nb6B9-GFP (cyan) and the Golgi marker (yellow), incubated with 10μM Dopamine.

Supplementary Movie 2. Confocal image series of D1DR expressing HEK293 cells (Magenta), Nb6B9-GFP (cyan) and the Golgi marker (yellow), incubated with 10μM Dopamine.

Supplementary Movie 3. Confocal image series of D1DR expressing HeLa cells (Magenta), Nb6B9-GFP (cyan) and the Golgi marker (yellow), incubated with 10μM SKF81927.

Supplementary Movie 4. Confocal image series of D1DR expressing HEK293 cells (Magenta), Nb6B9-GFP (cyan) and the Golgi marker (yellow), incubated with 10μM SKF81927.

Supplementary Movie 5. Confocal image series of D1DR expressing HEK293 cells (Magenta), Nb6B9-GFP (cyan) and OCT2-mApple (yellow), incubated with 10μM Dopamine.

Methods

Cell Culture, cDNA constructs and transfection

HeLa and HEK293 cells (purchased from ATCC as authenticated lines CCL-2, CRL-1573 and CRL 1446 respectively) were grown in Dulbecco's minimal essential medium supplemented with 10% Fetal Bovine Serum (FBS) without antibiotics. Cell cultures were free of mycoplasma contamination. Signal Sequence-Snap-tagged D1DR was created by amplifying D1DR from Flag-D1DR using 5'-GCCTGGGCTGGGTCTTGGATCCGATGACGCCATGGACG -3'; 5'-ATAGGGCCCTCTAGAGCCTCAGGTTGGGTGCTG -3' primers, and inserted into the Snap vector using BamHI and XbaI. pVenus-FRB-Nb6B9 was created by amplifying Nb6B9 and FRB from Nb6B9-GFP (30), and pC_4-R_HE plasmid (ARIAD Pharmaceuticals), using 5'-TGGTGGACAGGTGCAGCT -3'; 5'-GGATCCTCATGAGGAGACGGTGACCTGGGT -3' and 5'-GCTTCGAATTCAATCCTCTGGCAT -3'; 5'- TGCACCTGTCCACCAGCACTA-3 primers respectively, such that it contained the linker sequence GATAGTGCTGGTAGTGCTGGTGGAC, and inserted into the pVenus-C1 vector using EcoRI and BamH1. FKBP-GalT-mApple was created by amplifying FKBP and GalT from KDELr-FKBP and GalT-mCherry plasmids (a generous gift from Dr.Farese lab), using 5'-

CATGCTAGCGCCGCCACCATGGGAGTGCAGGTGGAAACCAT-3', 5'-GAGCTCGAGACCAGCACTACCAGCACTATCCTCCAGCTTCAGCAGCTCCACG3' and 5'- GCTCAAAGCTTGCCGCCACCGGAAGGCTTCGGGAGCCG-3', 5'-ACCGGATCCTTAGGCCCCTCCGGTCCGGAGCTCCCCG-3' primers, respectively and inserted into the pmApple-N1 vector using NheI, XhoI for FKBP and HindIII and BamHI for GalT(30). Transfections were performed using Lipofectamine 2000 (Invitrogen) according to the manufacturer's instructions. Snap tagged human D1DR constructs were labelled with Snap-cell 647 SiR (New England Biolabs, S9102S) as described previously (53).

Live-cell confocal imaging

Live cell imaging was carried out using Nikon spinning disk confocal microscope with a 60 ×, 1.4 numerical aperture, oil objective and a CO_2 and 37 °C temperature-controlled incubator. A 488, 568 nm and 640 Voltran was used as light sources for imaging GFP, mRFP/mApple, and Snap-647 signals, respectively. Cells expressing both Snap-tagged receptor (2µg) and the indicated nanobody–GFP (200ng) were plated onto glass coverslips. Receptors were surface labelled by addition of Snap-Cell 647 SiR (1:1000, New England Biolabs) to the media for 20 min, as described previously. Live cell images where endocytosis was inhibited were carried out by incubating the cells in 30µM Dyngo 4a (ab120689) at 37 °C for 30 minutes before indicated agonist was added. HEK293 PKA-Cat-GFP knock-in cells were a generous gift from the Huang Lab. Indicated agonist (dopamine hydrochloride-Sigma, SKF81297 hydrobromide-Tocris) were added and cells were imaged every 20 s for 20 min in DMEM without phenol red supplemented with 30 mM HEPES, pH 7.4. Time-lapse images were acquired with a CMOS camera (Photometrics) driven by Nikon Imaging Software (NS elements).

Fixed-cell confocal imaging

Cells were permeabilized with saponin to reduce the cytoplasmic background, as described previously(54). Briefly, MDCK cells were permeabilized with 0.05% saponin (Sigma) in PEM buffer (80mM K-Pipes, pH 6.8, 5 mM EGTA, 1mM MgCl2) for 5 min on ice. Cells were then fixed with 3% paraformaldehyde in PBS for 10 min and then quenched with 50mM Nh4Cl in PBS for 15 min. Primary antibodies (D1DR antibody (ab216644) 1:100, GM130 (BD biosciences 610822) (1:1000), and SLC22A2/OCT2 antibody (ab170871) were diluted in PBS supplemented with 0.05% saponin. Confocal images were taken using Nikon spinning disk confocal microscope with a 60x 1.4 numerical aperture, oil objective.

Image analysis and statistical analysis

Images were saved as 16-bit TIFF files. Quantitative image analysis was carried out on unprocessed images using ImageJ software (http://rsb.info.nih.gov/ij). For estimating kinetics of Nb6B9–GFP recruitment at the Golgi membrane over time in confocal images, individual cells were selected manually and average fluorescence intensity was measured at the Golgi area in each frame and normalized to the fluorescence intensity of D1DR at the Golgi. A blank area of the image lacking cells was used to estimate background fluorescence. For estimating kinetics of PKA-Cat GFP translocation from the Golgi

membrane over time in confocal images, individual cells were selected manually and average fluorescence intensity was measured at the Golgi area in each frame and normalized to the fluorescence intensity of the D1DR at the Golgi. A blank area of the image lacking cells was used to estimate background fluorescence. Co-localization analysis at the Golgi was estimated by calculating the Pearson's coefficient between the indicated image channels with the Golgi marker channel, using the co-localization plug-in for ImageJ (Coloc2). *P* values are from two-tailed unpaired Student's *t*-tests calculated using Prism 6.0 software (GraphPad Software).

Luminescence-based cAMP assay

HEK 293 cells stably expressing D1DR were transfected with a plasmid encoding a cyclic-permuted luciferase reporter construct, (pGloSensor-20F, Promega) and luminescence values were measured, as described previously(14). Briefly, cells were plated in 96-well dishes (~100,000 cells per well) in 500µl DMEM without phenol red/no serum and equilibrated to 37 °C in the SpectraMax plate reader and luminescence was measured every 1.5 min. Software was used to calculate integrated luminescence intensity and background subtraction. In rapamycin heterodimerization experiments, cells were pre-incubated with 1µM A/C heterodimerizer (Takara 635056) for 15 min. 5µM forskolin was used as a reference value in each multi-well plate and for each experimental condition. The average luminescence value (measured across duplicate wells) was normalized to the maximum luminescence value measured in the presence of 5µM forskolin. For rapamycin treated cells, the average luminescence value was normalized to the maximum luminescence value measured in the presence of 5µM forskolin and 1µM Rapamycin.

Western blotting

Cells from HEK293, HEK293T and HeLa were lysed in extraction buffer (0.2% Triton X-100, 50mM NaCl, 5mM EDTA, 50mM Tris at pH 7.4 and complete EDTA-free protease inhibitor cocktail (Roche). Extracts were mixed with SDS sample buffer for degradation. The proteins were resolved by SDS-PAGE and transferred to nitrocellulose membrane and blotted for anti-SLC22A2 (ab170871-1:1000) or GAPDH (1:10,000) antibodies to detect OCT2 and GAPDH expression by horseradish-peroxidase-conjugated rabbit IgG, sheep anti-mouse and rabbit IgG (1:10,000 Amersham Biosciences) and SuperSignal extended duration detection reagent (Pierce).

Data availability

Our research resources, including methods, cells and protocols are available upon request. All reagents developed, such as FRB and FKBP constructs, as well as detailed methods will be available upon request. The corresponding author adheres to the NIH Grants Policy and Sharing of Unique Research Resources.

Acknowledgments

We thank K. Silm, A. B. Lobingier, A. Manglik and D. Larsen for assistance, advice and valuable discussion. These studies were supported by the National Institute on General Medicine (GM133521) to R.I.

Author Contributions

N.P and G.R.R. designed experimental strategy, carried out all of the experiments and analysis. Q.N.M contributed to the cAMP experimental design and analysis. R.I. designed the experimental strategy, contributed to interpreting the results and writing the paper.

Competing financial interests

The authors declare no competing financial interests.

References

1. Missale C, Nash SR, Robinson SW, Jaber M, Caron MG. Dopamine receptors: from structure to function. Physiol Rev. 1998;78(1):189-225. Epub 1998/02/11. doi: 10.1152/physrev.1998.78.1.189. PubMed PMID: 9457173.
2. Wang J, Hanada K, Staus DP, Makara MA, Dahal GR, Chen Q, Ahles A, Engelhardt S, Rockman HA. Galphai is required for carvedilol-induced beta1 adrenergic receptor beta-arrestin biased signaling. Nat Commun. 2017;8(1):1706. Epub 2017/11/24. doi: 10.1038/s41467-017-01855-z. PubMed PMID: 29167435; PMCID: PMC5700200.
3. Agarwal SR, MacDougall DA, Tyser R, Pugh SD, Calaghan SC, Harvey RD. Effects of cholesterol depletion on compartmentalized cAMP responses in adult cardiac myocytes. J Mol Cell Cardiol. 2011;50(3):500-9. Epub 2010/12/01. doi: 10.1016/j.yjmcc.2010.11.015. PubMed PMID: 21115018; PMCID: PMC3049871.
4. Kebabian JW. Dopamine-sensitive adenylyl cyclase: a receptor mechanism for dopamine. Adv Biochem Psychopharmacol. 1978;19:131-54. Epub 1978/01/01. PubMed PMID: 29445.
5. Spano PF, Govoni S, Trabucchi M. Studies on the pharmacological properties of dopamine receptors in various areas of the central nervous system. Adv Biochem Psychopharmacol. 1978;19:155-65. Epub 1978/01/01. PubMed PMID: 358777.
6. Beaulieu JM, Espinoza S, Gainetdinov RR. Dopamine receptors - IUPHAR Review 13. Br J Pharmacol. 2015;172(1):1-23. Epub 2015/02/12. doi: 10.1111/bph.12906. PubMed PMID: 25671228; PMCID: PMC4280963.
7. Ariano MA, Sortwell CE, Ray M, Altemus KL, Sibley DR, Levine MS. Agonist-induced morphologic decrease in cellular D1A dopamine receptor staining. Synapse. 1997;27(4):313-21. Epub 1998/02/12. doi: 10.1002/(SICI)1098-2396(199712)27:4<313::AID-SYN5>3.0.CO;2-F. PubMed PMID: 9372554.
8. Bloch B, Bernard V, Dumartin B. "In vivo" intraneuronal trafficking of G protein coupled receptors in the striatum: regulation by dopaminergic and cholinergic environment. Biol Cell. 2003;95(7):477-88. Epub 2003/11/05. doi: 10.1016/s0248-4900(03)00080-7. PubMed PMID: 14597266.
9. Vickery RG, von Zastrow M. Distinct dynamin-dependent and -independent mechanisms target structurally homologous dopamine receptors to different endocytic membranes. J Cell Biol. 1999;144(1):31-43. Epub 1999/01/13. doi: 10.1083/jcb.144.1.31. PubMed PMID: 9885242; PMCID: PMC2148123.

10. Calebiro D, Nikolaev VO, Lohse MJ. Imaging of persistent cAMP signaling by internalized G protein-coupled receptors. J Mol Endocrinol. 2010;45(1):1-8. Epub 2010/04/10. doi: 10.1677/JME-10-0014. PubMed PMID: 20378719.
11. Ferrandon S, Feinstein TN, Castro M, Wang B, Bouley R, Potts JT, Gardella TJ, Vilardaga JP. Sustained cyclic AMP production by parathyroid hormone receptor endocytosis. Nat Chem Biol. 2009;5(10):734-42. Epub 2009/08/25. doi: 10.1038/nchembio.206. PubMed PMID: 19701185; PMCID: PMC3032084.
12. Feinstein TN, Yui N, Webber MJ, Wehbi VL, Stevenson HP, King JD, Jr., Hallows KR, Brown D, Bouley R, Vilardaga JP. Noncanonical control of vasopressin receptor type 2 signaling by retromer and arrestin. J Biol Chem. 2013;288(39):27849-60. Epub 2013/08/13. doi: 10.1074/jbc.M112.445098. PubMed PMID: 23935101; PMCID: PMC3784700.
13. Kotowski SJ, Hopf FW, Seif T, Bonci A, von Zastrow M. Endocytosis promotes rapid dopaminergic signaling. Neuron. 2011;71(2):278-90. Epub 2011/07/28. doi: 10.1016/j.neuron.2011.05.036. PubMed PMID: 21791287; PMCID: PMC3417347.
14. Irannejad R, Tomshine JC, Tomshine JR, Chevalier M, Mahoney JP, Steyaert J, Rasmussen SG, Sunahara RK, El-Samad H, Huang B, von Zastrow M. Conformational biosensors reveal GPCR signalling from endosomes. Nature. 2013;495(7442):534-8. Epub 2013/03/22. doi: 10.1038/nature12000. PubMed PMID: 23515162; PMCID: PMC3835555.
15. Irannejad R, von Zastrow M. GPCR signaling along the endocytic pathway. Curr Opin Cell Biol. 2014;27:109-16. Epub 2014/04/01. doi: 10.1016/j.ceb.2013.10.003. PubMed PMID: 24680436; PMCID: PMC4968408.
16. Irannejad R, Tsvetanova NG, Lobingier BT, von Zastrow M. Effects of endocytosis on receptor-mediated signaling. Curr Opin Cell Biol. 2015;35:137-43. Epub 2015/06/10. doi: 10.1016/j.ceb.2015.05.005. PubMed PMID: 26057614; PMCID: PMC4529812.
17. Thomsen ARB, Jensen DD, Hicks GA, Bunnett NW. Therapeutic Targeting of Endosomal G-Protein-Coupled Receptors. Trends Pharmacol Sci. 2018;39(10):879-91. Epub 2018/09/06. doi: 10.1016/j.tips.2018.08.003. PubMed PMID: 30180973; PMCID: PMC6508874.
18. Calebiro D, Koszegi Z. The subcellular dynamics of GPCR signaling. Mol Cell Endocrinol. 2019;483:24-30. Epub 2019/01/06. doi: 10.1016/j.mce.2018.12.020. PubMed PMID: 30610913.
19. Lobingier BT, von Zastrow M. When trafficking and signaling mix: How subcellular location shapes G protein-coupled receptor activation of heterotrimeric G proteins. Traffic. 2019;20(2):130-6. Epub 2018/12/24. doi: 10.1111/tra.12634. PubMed PMID: 30578610; PMCID: PMC6387827.
20. Stoeber M, Jullie D, Lobingier BT, Laeremans T, Steyaert J, Schiller PW, Manglik A, von Zastrow M. A Genetically Encoded Biosensor Reveals Location Bias of Opioid Drug Action. Neuron. 2018;98(5):963-76 e5. Epub 2018/05/15. doi: 10.1016/j.neuron.2018.04.021. PubMed PMID: 29754753; PMCID: PMC6481295.
21. Tsvetanova NG, von Zastrow M. Spatial encoding of cyclic AMP signaling specificity by GPCR endocytosis. Nat Chem Biol. 2014;10(12):1061-5. Epub 2014/11/05. doi: 10.1038/nchembio.1665. PubMed PMID: 25362359; PMCID: PMC4232470.
22. Bowman SL, Shiwarski DJ, Puthenveedu MA. Distinct G protein-coupled receptor recycling pathways allow spatial control of downstream G protein signaling. J Cell Biol.

2016;214(7):797-806. Epub 2016/09/21. doi: 10.1083/jcb.201512068. PubMed PMID: 27646272; PMCID: PMC5037407.
23. Jensen DD, Lieu T, Halls ML, Veldhuis NA, Imlach WL, Mai QN, Poole DP, Quach T, Aurelio L, Conner J, Herenbrink CK, Barlow N, Simpson JS, Scanlon MJ, Graham B, McCluskey A, Robinson PJ, Escriou V, Nassini R, Materazzi S, Geppetti P, Hicks GA, Christie MJ, Porter CJH, Canals M, Bunnett NW. Neurokinin 1 receptor signaling in endosomes mediates sustained nociception and is a viable therapeutic target for prolonged pain relief. Sci Transl Med. 2017;9(392). Epub 2017/06/02. doi: 10.1126/scitranslmed.aal3447. PubMed PMID: 28566424; PMCID: PMC6034632.
24. Godbole A, Lyga S, Lohse MJ, Calebiro D. Internalized TSH receptors en route to the TGN induce local Gs-protein signaling and gene transcription. Nat Commun. 2017;8(1):443. Epub 2017/09/07. doi: 10.1038/s41467-017-00357-2. PubMed PMID: 28874659; PMCID: PMC5585343.
25. Jean-Alphonse F, Bowersox S, Chen S, Beard G, Puthenveedu MA, Hanyaloglu AC. Spatially restricted G protein-coupled receptor activity via divergent endocytic compartments. J Biol Chem. 2014;289(7):3960-77. Epub 2014/01/01. doi: 10.1074/jbc.M113.526350. PubMed PMID: 24375413; PMCID: PMC3924264.
26. Bock A, Annibale P, Konrad C, Hannawacker A, Anton SE, Maiellaro I, Zabel U, Sivaramakrishnan S, Falcke M, Lohse MJ. Optical Mapping of cAMP Signaling at the Nanometer Scale. Cell. 2020;182(6):1519-30 e17. Epub 2020/08/28. doi: 10.1016/j.cell.2020.07.035. PubMed PMID: 32846156.
27. Saucerman JJ, Greenwald EC, Polanowska-Grabowska R. Mechanisms of cyclic AMP compartmentation revealed by computational models. J Gen Physiol. 2014;143(1):39-48. Epub 2014/01/01. doi: 10.1085/jgp.201311044. PubMed PMID: 24378906; PMCID: PMC3874575.
28. Richards M, Lomas O, Jalink K, Ford KL, Vaughan-Jones RD, Lefkimmiatis K, Swietach P. Intracellular tortuosity underlies slow cAMP diffusion in adult ventricular myocytes. Cardiovasc Res. 2016;110(3):395-407. Epub 2016/04/20. doi: 10.1093/cvr/cvw080. PubMed PMID: 27089919; PMCID: PMC4872880.
29. Agarwal SR, Clancy CE, Harvey RD. Mechanisms Restricting Diffusion of Intracellular cAMP. Sci Rep. 2016;6:19577. Epub 2016/01/23. doi: 10.1038/srep19577. PubMed PMID: 26795432; PMCID: PMC4726171.
30. Irannejad R, Pessino V, Mika D, Huang B, Wedegaertner PB, Conti M, von Zastrow M. Functional selectivity of GPCR-directed drug action through location bias. Nat Chem Biol. 2017;13(7):799-806. Epub 2017/05/30. doi: 10.1038/nchembio.2389. PubMed PMID: 28553949; PMCID: PMC5733145.
31. Nash CA, Wei W, Irannejad R, Smrcka AV. Golgi localized beta1-adrenergic receptors stimulate Golgi PI4P hydrolysis by PLCepsilon to regulate cardiac hypertrophy. Elife. 2019;8. Epub 2019/08/23. doi: 10.7554/eLife.48167. PubMed PMID: 31433293; PMCID: PMC6726460.
32. Rasmussen SG, Choi HJ, Fung JJ, Pardon E, Casarosa P, Chae PS, Devree BT, Rosenbaum DM, Thian FS, Kobilka TS, Schnapp A, Konetzki I, Sunahara RK, Gellman SH, Pautsch A, Steyaert J, Weis WI, Kobilka BK. Structure of a nanobody-stabilized active state of the beta(2) adrenoceptor. Nature. 2011;469(7329):175-80. Epub 2011/01/14. doi: 10.1038/nature09648. PubMed PMID: 21228869; PMCID: PMC3058308.

33. Ring AM, Manglik A, Kruse AC, Enos MD, Weis WI, Garcia KC, Kobilka BK. Adrenaline-activated structure of beta2-adrenoceptor stabilized by an engineered nanobody. Nature. 2013;502(7472):575-9. Epub 2013/09/24. doi: 10.1038/nature12572. PubMed PMID: 24056936; PMCID: PMC3822040.
34. Wan Q, Okashah N, Inoue A, Nehme R, Carpenter B, Tate CG, Lambert NA. Mini G protein probes for active G protein-coupled receptors (GPCRs) in live cells. J Biol Chem. 2018;293(19):7466-73. Epub 2018/03/11. doi: 10.1074/jbc.RA118.001975. PubMed PMID: 29523687; PMCID: PMC5949987.
35. Taubert D, Grimberg G, Stenzel W, Schomig E. Identification of the endogenous key substrates of the human organic cation transporter OCT2 and their implication in function of dopaminergic neurons. PLoS One. 2007;2(4):e385. Epub 2007/04/27. doi: 10.1371/journal.pone.0000385. PubMed PMID: 17460754; PMCID: PMC1851987.
36. Busch AE, Karbach U, Miska D, Gorboulev V, Akhoundova A, Volk C, Arndt P, Ulzheimer JC, Sonders MS, Baumann C, Waldegger S, Lang F, Koepsell H. Human neurons express the polyspecific cation transporter hOCT2, which translocates monoamine neurotransmitters, amantadine, and memantine. Mol Pharmacol. 1998;54(2):342-52. Epub 1998/08/04. doi: 10.1124/mol.54.2.342. PubMed PMID: 9687576.
37. Bednarczyk D, Ekins S, Wikel JH, Wright SH. Influence of molecular structure on substrate binding to the human organic cation transporter, hOCT1. Mol Pharmacol. 2003;63(3):489-98. Epub 2003/02/28. doi: 10.1124/mol.63.3.489. PubMed PMID: 12606755.
38. Amphoux A, Vialou V, Drescher E, Bruss M, Mannoury La Cour C, Rochat C, Millan MJ, Giros B, Bonisch H, Gautron S. Differential pharmacological in vitro properties of organic cation transporters and regional distribution in rat brain. Neuropharmacology. 2006;50(8):941-52. Epub 2006/04/04. doi: 10.1016/j.neuropharm.2006.01.005. PubMed PMID: 16581093.
39. Cancino J, Capalbo A, Di Campli A, Giannotta M, Rizzo R, Jung JE, Di Martino R, Persico M, Heinklein P, Sallese M, Luini A. Control systems of membrane transport at the interface between the endoplasmic reticulum and the Golgi. Dev Cell. 2014;30(3):280-94. Epub 2014/08/15. doi: 10.1016/j.devcel.2014.06.018. PubMed PMID: 25117681.
40. Boivin B, Lavoie C, Vaniotis G, Baragli A, Villeneuve LR, Ethier N, Trieu P, Allen BG, Hebert TE. Functional beta-adrenergic receptor signalling on nuclear membranes in adult rat and mouse ventricular cardiomyocytes. Cardiovasc Res. 2006;71(1):69-78. Epub 2006/04/25. doi: 10.1016/j.cardiores.2006.03.015. PubMed PMID: 16631628.
41. Chung KY, Rasmussen SG, Liu T, Li S, DeVree BT, Chae PS, Calinski D, Kobilka BK, Woods VL, Jr., Sunahara RK. Conformational changes in the G protein Gs induced by the beta2 adrenergic receptor. Nature. 2011;477(7366):611-5. Epub 2011/10/01. doi: 10.1038/nature10488. PubMed PMID: 21956331; PMCID: PMC3448949.
42. Soberg K, Skalhegg BS. The Molecular Basis for Specificity at the Level of the Protein Kinase a Catalytic Subunit. Front Endocrinol (Lausanne). 2018;9:538. Epub 2018/09/28. doi: 10.3389/fendo.2018.00538. PubMed PMID: 30258407; PMCID: PMC6143667.
43. Nigg EA, Schafer G, Hilz H, Eppenberger HM. Cyclic-AMP-dependent protein kinase type II is associated with the Golgi complex and with centrosomes. Cell.

1985;41(3):1039-51. Epub 1985/07/01. doi: 10.1016/s0092-8674(85)80084-2. PubMed PMID: 2988780.
44. Tillo SE, Xiong WH, Takahashi M, Miao S, Andrade AL, Fortin DA, Yang G, Qin M, Smoody BF, Stork PJS, Zhong H. Liberated PKA Catalytic Subunits Associate with the Membrane via Myristoylation to Preferentially Phosphorylate Membrane Substrates. Cell Rep. 2017;19(3):617-29. Epub 2017/04/20. doi: 10.1016/j.celrep.2017.03.070. PubMed PMID: 28423323; PMCID: PMC5481286.
45. Walker-Gray R, Stengel F, Gold MG. Mechanisms for restraining cAMP-dependent protein kinase revealed by subunit quantitation and cross-linking approaches. Proc Natl Acad Sci U S A. 2017;114(39):10414-9. Epub 2017/09/13. doi: 10.1073/pnas.1701782114. PubMed PMID: 28893983; PMCID: PMC5625894.
46. Buxton IL, Brunton LL. Compartments of cyclic AMP and protein kinase in mammalian cardiomyocytes. J Biol Chem. 1983;258(17):10233-9. Epub 1983/09/10. PubMed PMID: 6309796.
47. Warrier S, Ramamurthy G, Eckert RL, Nikolaev VO, Lohse MJ, Harvey RD. cAMP microdomains and L-type Ca2+ channel regulation in guinea-pig ventricular myocytes. J Physiol. 2007;580(Pt.3):765-76. Epub 2007/02/10. doi: 10.1113/jphysiol.2006.124891. PubMed PMID: 17289786; PMCID: PMC2075464.
48. Steinberg SF, Brunton LL. Compartmentation of G protein-coupled signaling pathways in cardiac myocytes. Annu Rev Pharmacol Toxicol. 2001;41:751-73. Epub 2001/03/27. doi: 10.1146/annurev.pharmtox.41.1.751. PubMed PMID: 11264475.
49. Musheshe N, Schmidt M, Zaccolo M. cAMP: From Long-Range Second Messenger to Nanodomain Signalling. Trends Pharmacol Sci. 2018;39(2):209-22. Epub 2018/01/01. doi: 10.1016/j.tips.2017.11.006. PubMed PMID: 29289379.
50. Gold MG, Gonen T, Scott JD. Local cAMP signaling in disease at a glance. J Cell Sci. 2013;126(Pt 20):4537-43. Epub 2013/10/15. doi: 10.1242/jcs.133751. PubMed PMID: 24124191; PMCID: PMC3795333.
51. Double KL, Crocker AD. Dopamine receptors in the substantia nigra are involved in the regulation of muscle tone. Proc Natl Acad Sci U S A. 1995;92(5):1669-73. Epub 1995/02/28. doi: 10.1073/pnas.92.5.1669. PubMed PMID: 7878037; PMCID: PMC42581.
52. Arnsten AF, Cai JX, Steere JC, Goldman-Rakic PS. Dopamine D2 receptor mechanisms contribute to age-related cognitive decline: the effects of quinpirole on memory and motor performance in monkeys. J Neurosci. 1995;15(5 Pt 1):3429-39. Epub 1995/05/01. PubMed PMID: 7751922; PMCID: PMC6578230.
53. Lukinavicius G, Umezawa K, Olivier N, Honigmann A, Yang G, Plass T, Mueller V, Reymond L, Correa IR, Jr., Luo ZG, Schultz C, Lemke EA, Heppenstall P, Eggeling C, Manley S, Johnsson K. A near-infrared fluorophore for live-cell super-resolution microscopy of cellular proteins. Nat Chem. 2013;5(2):132-9. Epub 2013/01/25. doi: 10.1038/nchem.1546. PubMed PMID: 23344448.
54. Lobert VH, Stenmark H. The ESCRT machinery mediates polarization of fibroblasts through regulation of myosin light chain. J Cell Sci. 2012;125(Pt 1):29-36. Epub 2012/01/24. doi: 10.1242/jcs.088310. PubMed PMID: 22266905.

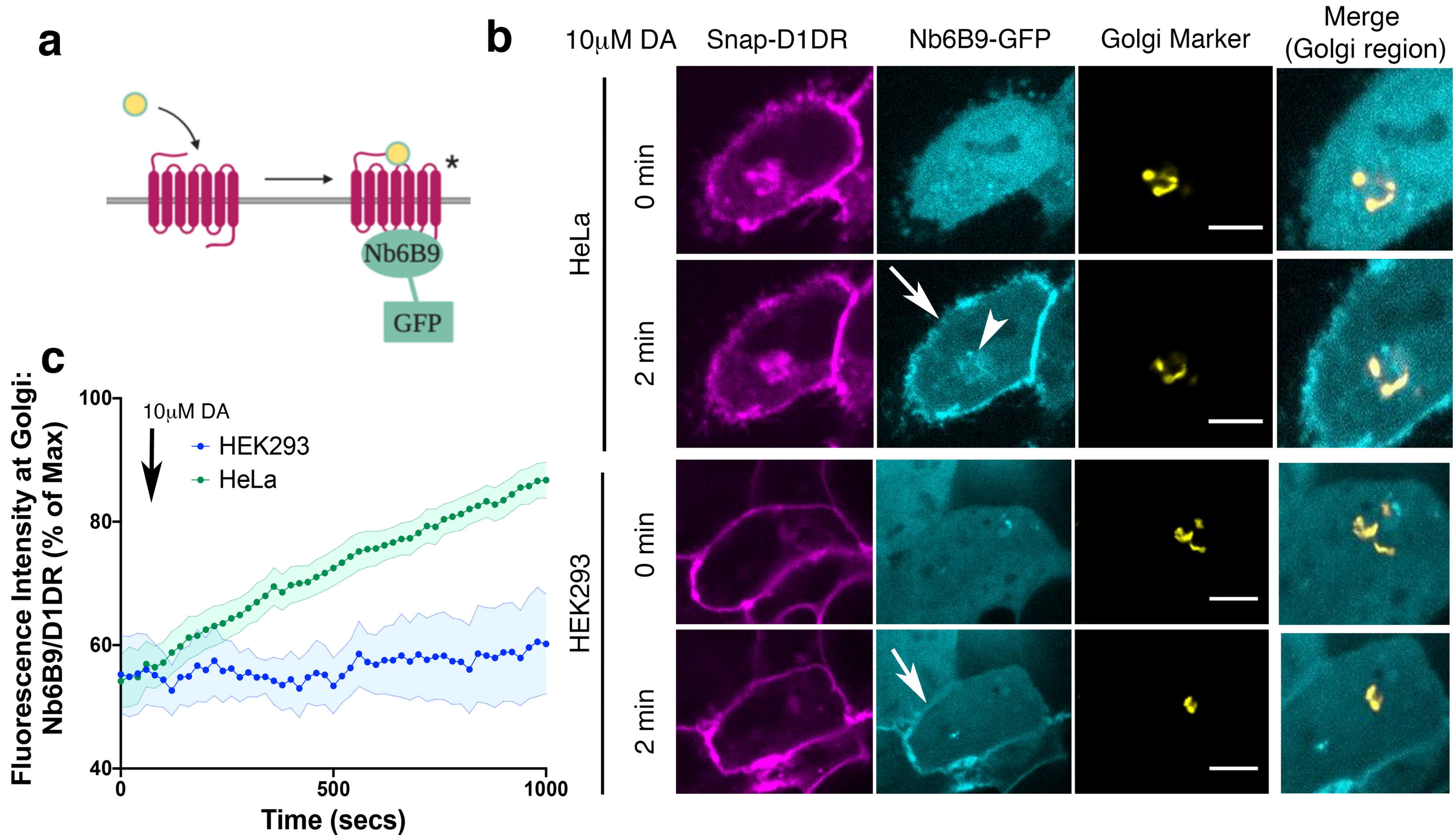
a
Nb6B9
GFP
*
b
10μM DA
Snap-D1DR
Nb6B9-GFP
Golgi Marker
Merge
(Golgi region)
HeLa
0 min
2 min
HEK293
0 min
2 min
c
10μM DA
HEK293
HeLa
Fluorescence Intensity at Golgi:
Nb6B9/D1DR (% of Max)
100
80
60
40
0
500
1000
Time (secs)

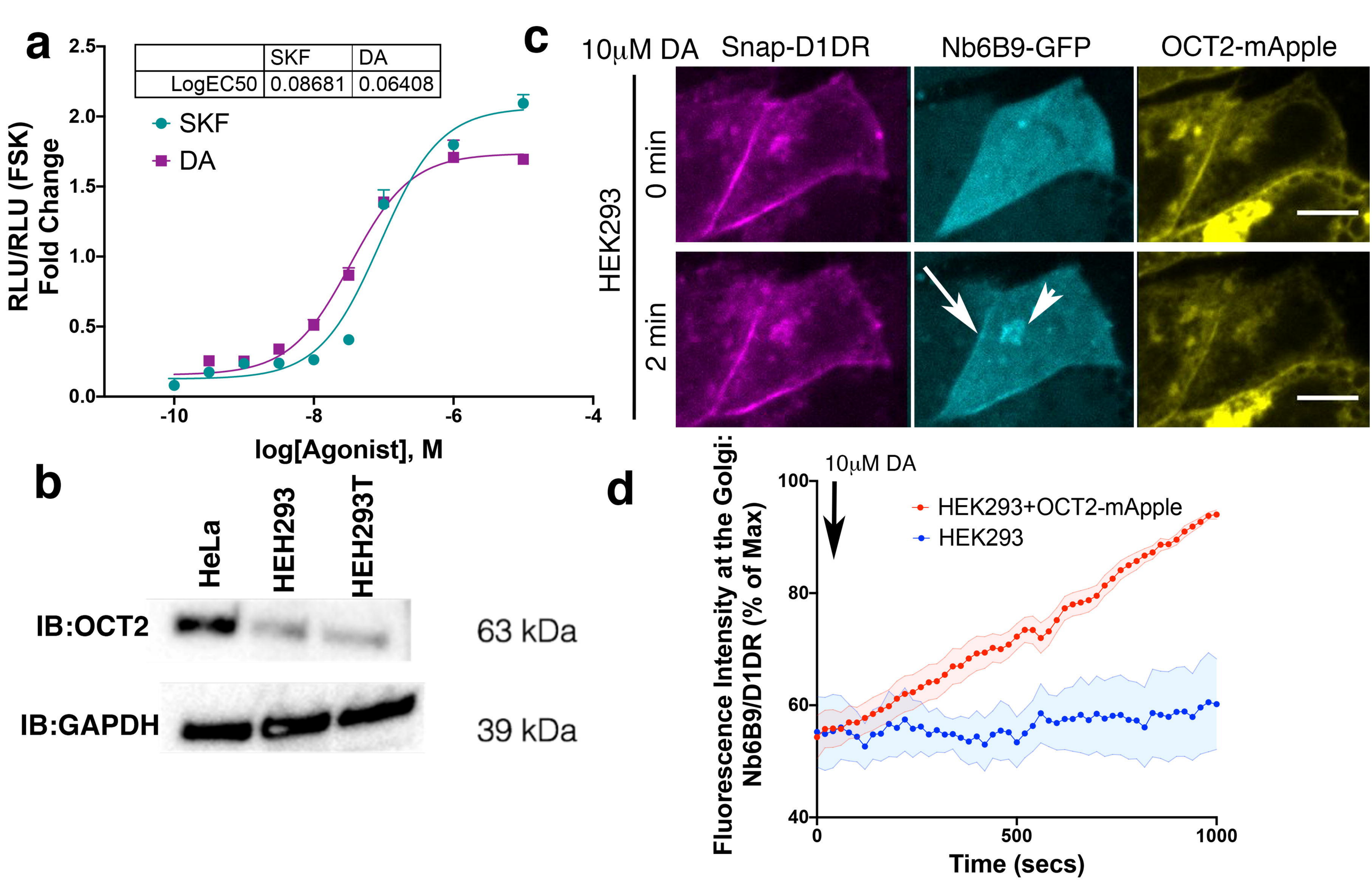
a
SKF
DA
LogEC50
0.08681
0.06408
SKF
DA
RLU/RLU (FSK)
Fold Change
2.5
2.0
1.5
1.0
0.5
0.0
-10
-8
-6
-4
log[Agonist], M
b
HeLa
HEH293
HEH293T
IB:OCT2
63 kDa
IB:GAPDH
39 kDa
c
10μM DA
Snap-D1DR
Nb6B9-GFP
OCT2-mApple
HEK293
0 min
2 min
d
10μM DA
HEK293+OCT2-mApple
HEK293
Fluorescence Intensity at the Golgi:
Nb6B9/D1DR (% of Max)
100
80
60
40
0
500
1000
Time (secs)

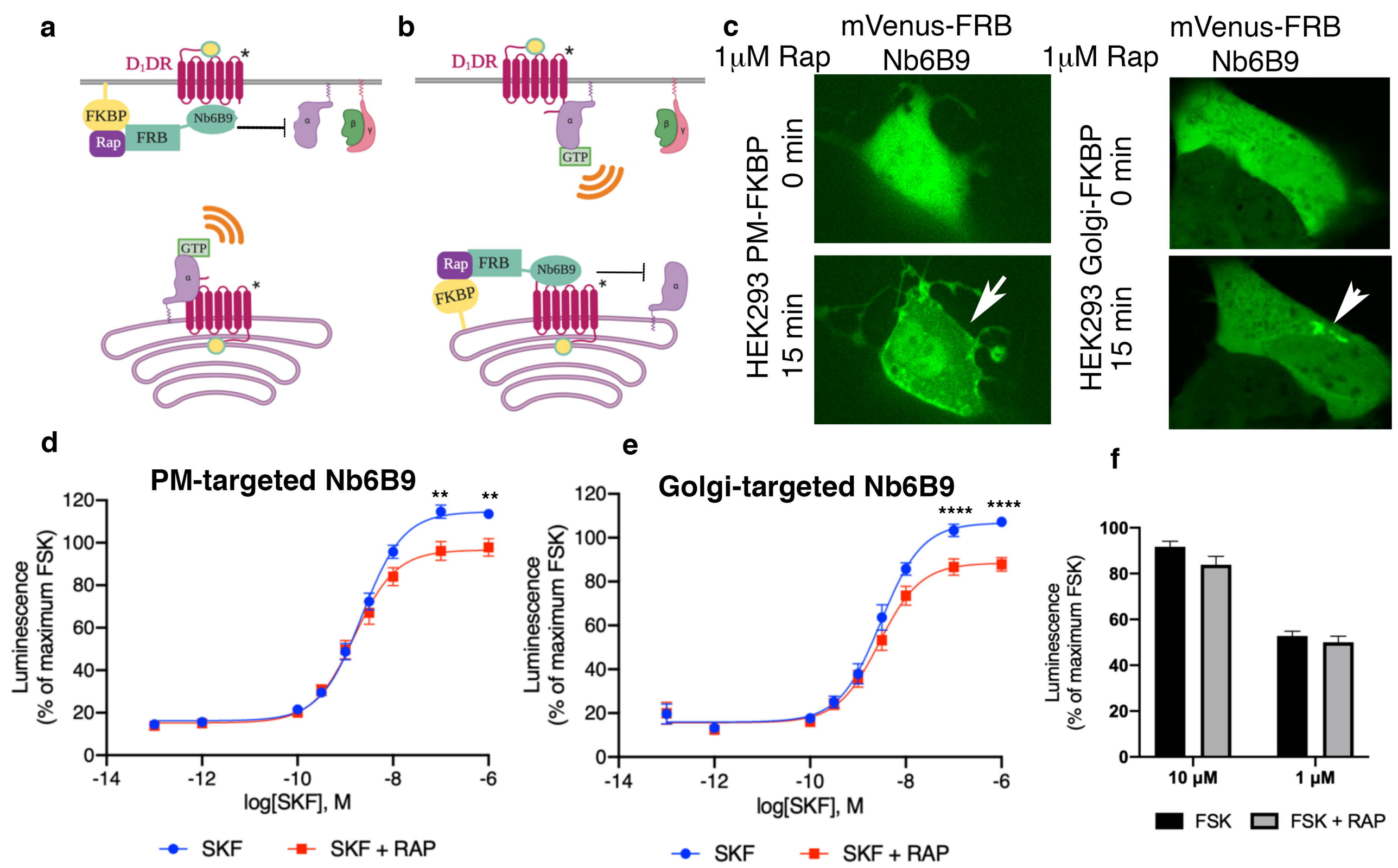
a
D1DR
FKBP
Rap
FRB
Nb6B9
α
β
γ
GTP
b
D1DR
GTP
Rap
FRB
Nb6B9
FKBP
c
1μM Rap
mVenus-FRB
Nb6B9
1μM Rap
mVenus-FRB
Nb6B9
HEK293 PM-FKBP
0 min
15 min
HEK293 Golgi-FKBP
0 min
15 min
d
PM-targeted Nb6B9
Luminescence
(% of maximum FSK)
log[SKF], M
SKF
SKF + RAP
e
Golgi-targeted Nb6B9
Luminescence
(% of maximum FSK)
log[SKF], M
SKF
SKF + RAP
f
Luminescence
(% of maximum FSK)
10 μM
1 μM
FSK
FSK + RAP

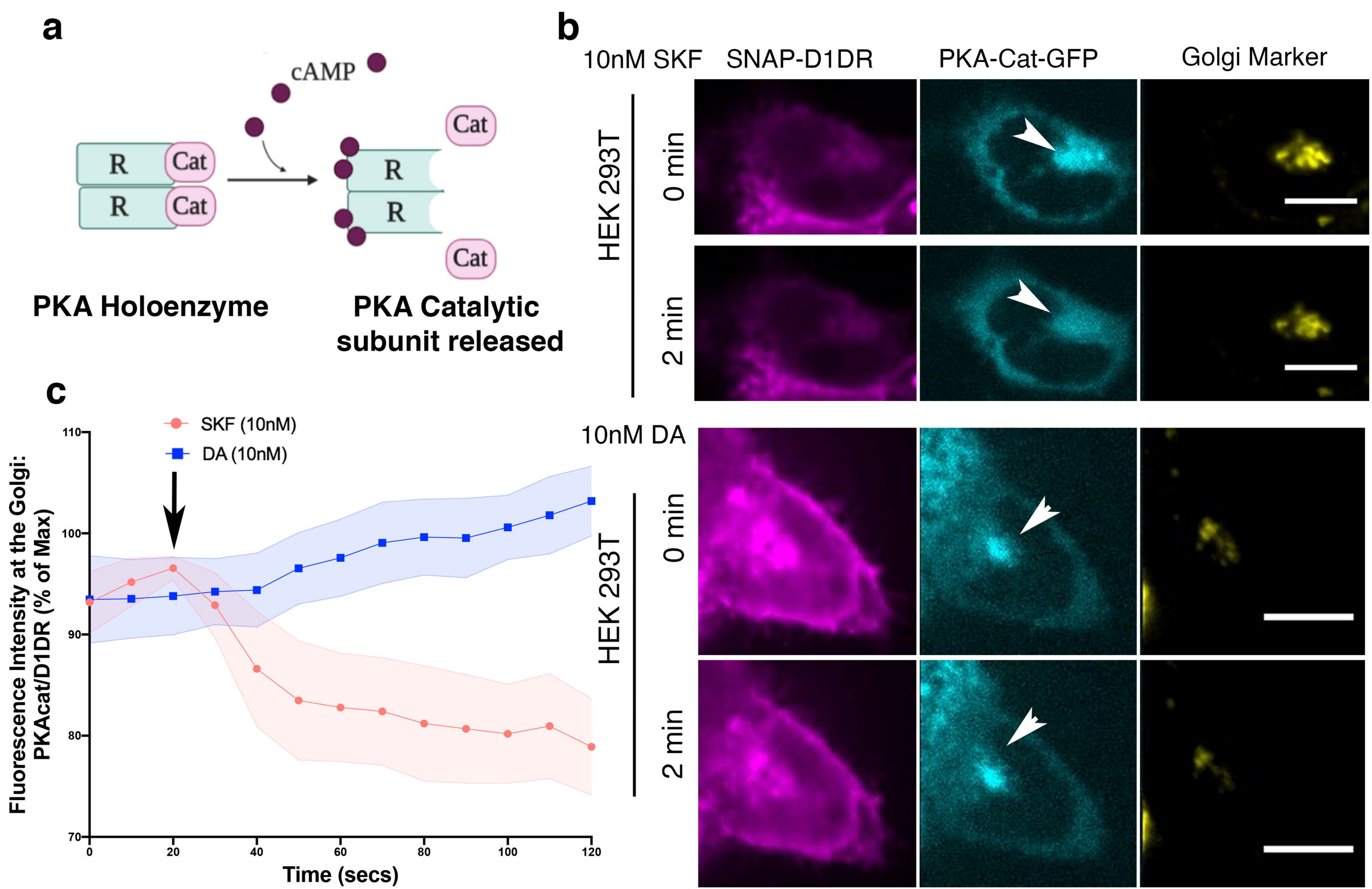
a
cAMP
R
Cat
R
Cat
R
R
Cat
Cat
PKA Holoenzyme
PKA Catalytic subunit released
b
10nM SKF
SNAP-D1DR
PKA-Cat-GFP
Golgi Marker
HEK 293T
0 min
2 min
10nM DA
HEK 293T
0 min
2 min
c
SKF (10nM)
DA (10nM)
Fluorescence Intensity at the Golgi: PKAcat/D1DR (% of Max)
110
100
90
80
70
0
20
40
60
80
100
120
Time (secs)

```
D1DR   17   ERDFSVRILTACFLSLLILSTLLGNTLVCAAVIRFRHLRSKVTNFFVISLAVSDLLVAVL  76
β2AR   27   ERDEVWVVGMGIVMSLIVLAIVFGNVLVITAIAKFERLQT-VTNYFITSLACADLVMGLA  85

D1DR   77   VMPWKAVAEIAGFWPFGSF-CNIWVAFDIMCSTASILNLCVISVDRYWAISSPFRYERKM  135
β2AR   86   VVPFGAAHILMKMWTFGNFWCEFWTSIDVLCVTASIETLCVIAVDRYFAITSPFKYQSLL  145

D1DR   136  TPKAAFILISVAWTLSVLISFIPVQLSWHKAKPTSPSDGNATSLAETIDNCDSSLSRTYA  195
β2AR   146  TKNKARVIILMVWIVSGLTSFLPIQMHWYRATHQEAINCYANETC-----CDFFTNQAYA  200

D1DR   196  ISSSVISFYIPVAIMIVTYTRIYRIAQKQIRRIAALERAAVHAKNCQTTTGNGKPVECSQ  255
β2AR   201  IASSIVSFYVPLVIMVFVYSRVFQEAKRQLQKIDKSE-GRFHVQNLSQVEQDGRTGHGLR  259

D1DR   256  PESSFKMSFKRETKVLKTLSVIMGVFVCCWLPFFILNCILPFCGSGETQPFCIDSNTFDV  315
β2AR   260  RSSKFCL---KEHKALKTLGIIMGTFTLCWLPFFIVNIVHVI------QDNLIRKEVYIL  310

D1DR   316  FVWFGWANSSLNPIIYAFNADFRKAFSTLLGCYR  349
β2AR   311  LNWIGYVNSGFNPLIYCRSPDFRIAFQELL-CLR  343
```

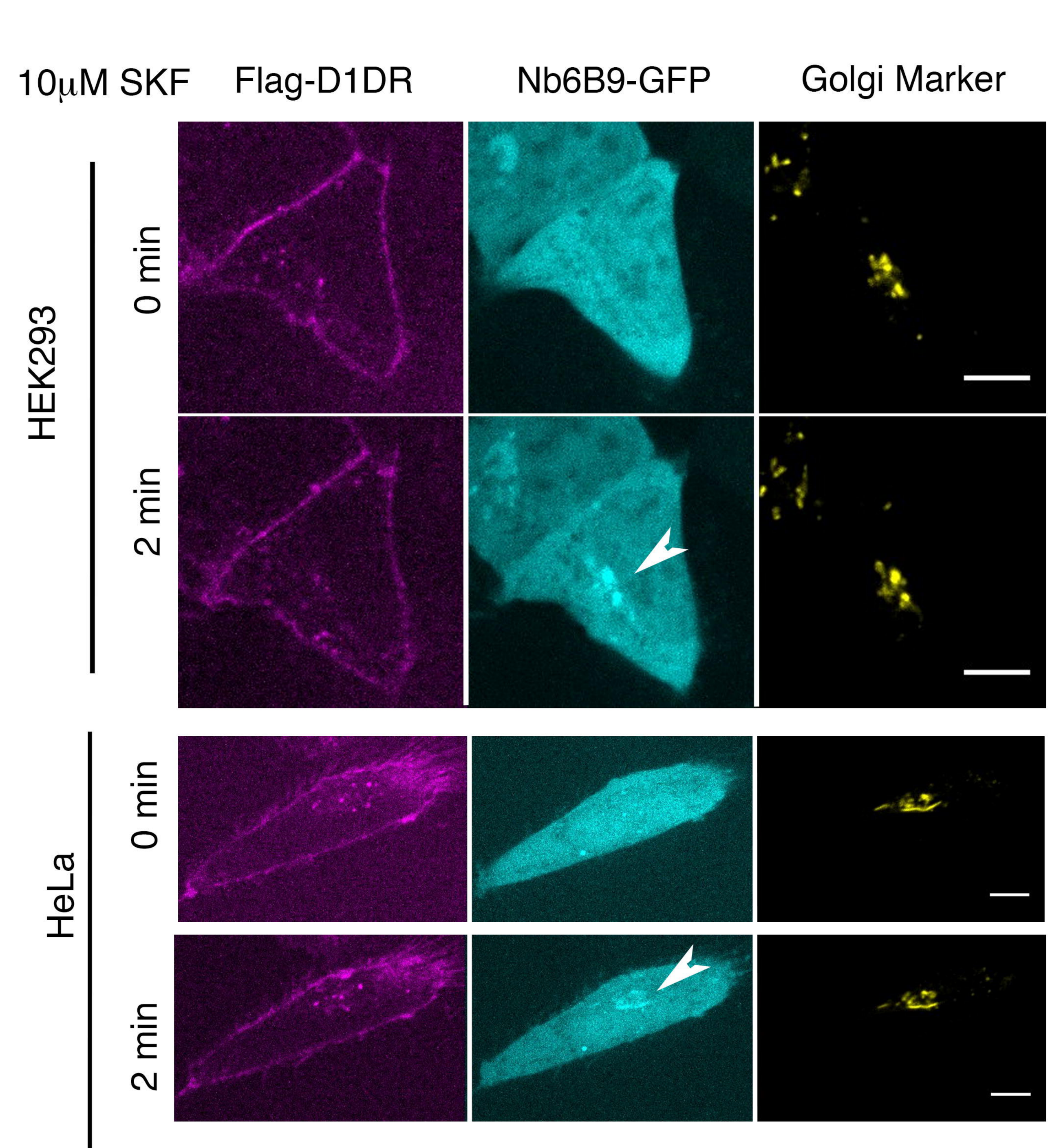
10μM SKF
Flag-D1DR
Nb6B9-GFP
Golgi Marker
HEK293
0 min
2 min
HeLa
0 min
2 min

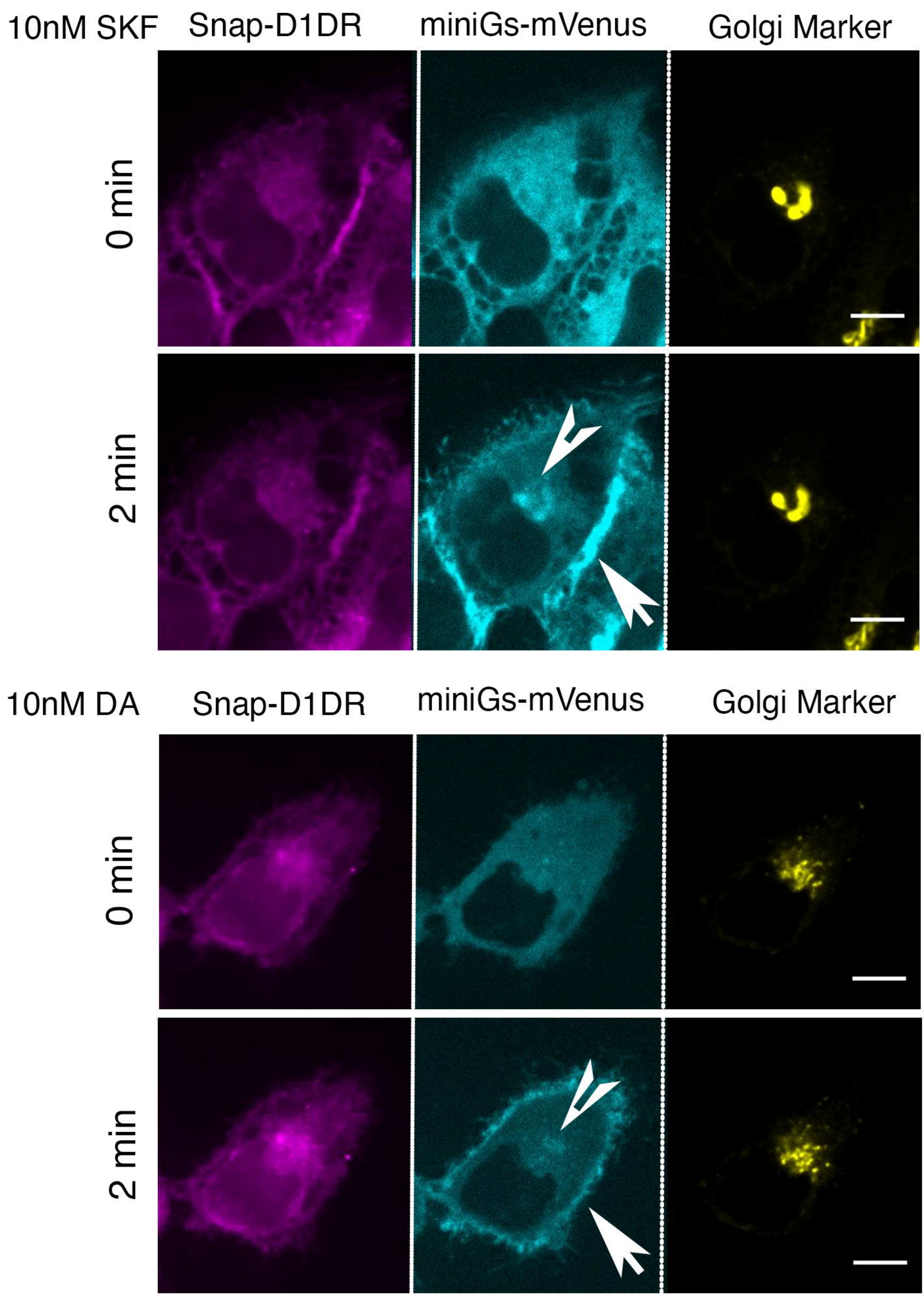
10nM SKF
Snap-D1DR
miniGs-mVenus
Golgi Marker
0 min
2 min
10nM DA
Snap-D1DR
miniGs-mVenus
Golgi Marker
0 min
2 min

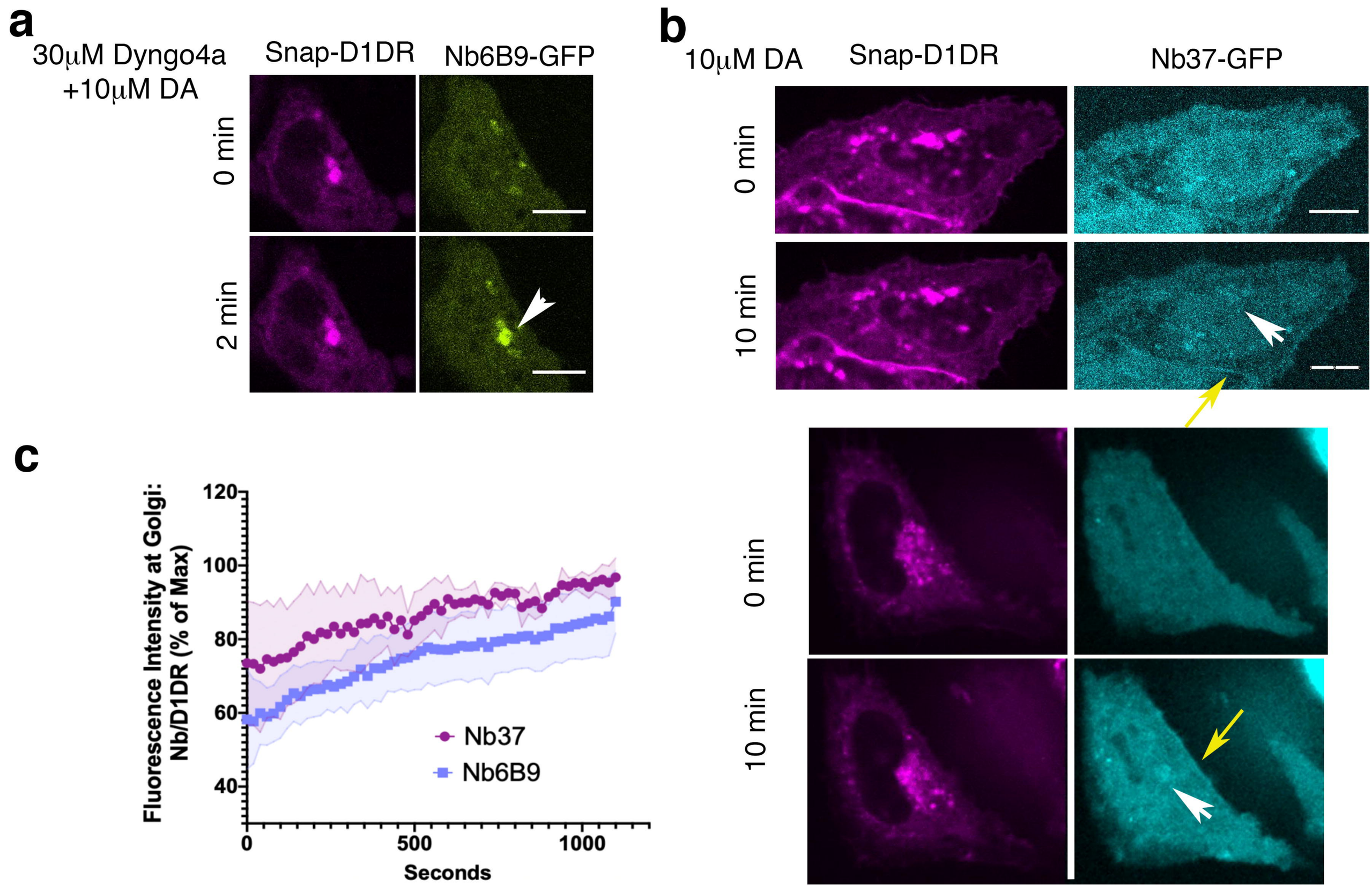
a
30μM Dyngo4a
+10μM DA
Snap-D1DR
Nb6B9-GFP
0 min
2 min
b
10μM DA
Snap-D1DR
Nb37-GFP
0 min
10 min
c
Fluorescence Intensity at Golgi:
Nb/D1DR (% of Max)
120
100
80
60
40
0
500
1000
Seconds
Nb37
Nb6B9
0 min
10 min

a

D1DR antibody | GM130 | Merge

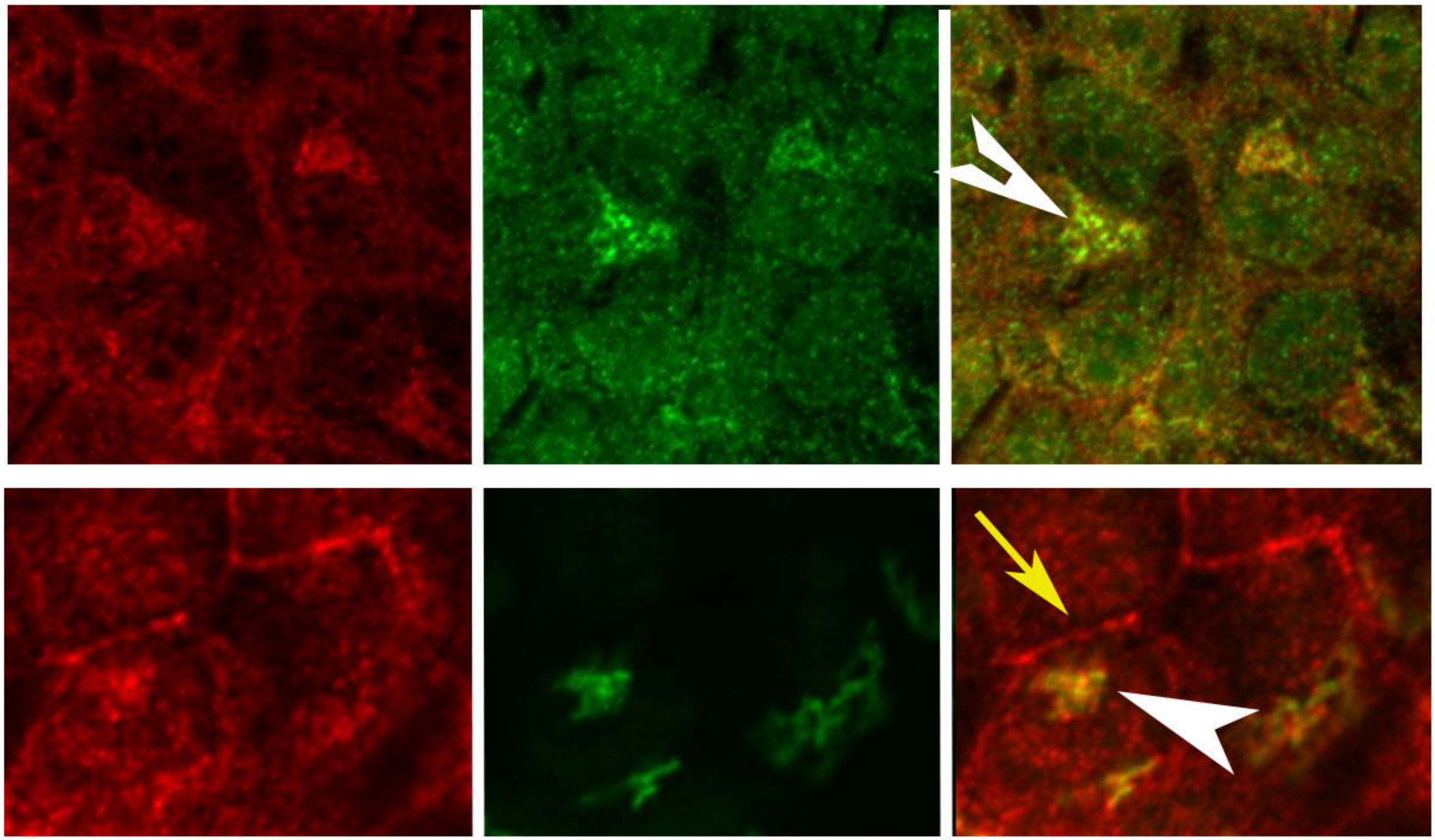

b

OCT2 antibody | GM130 | Merge

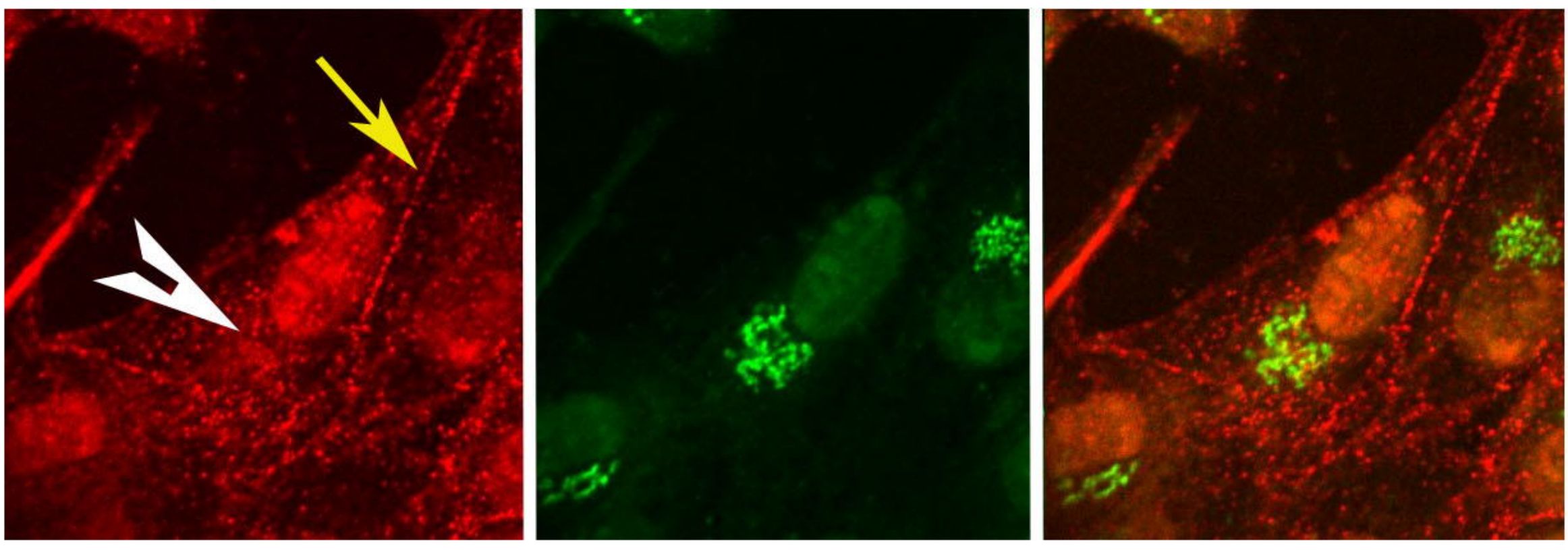

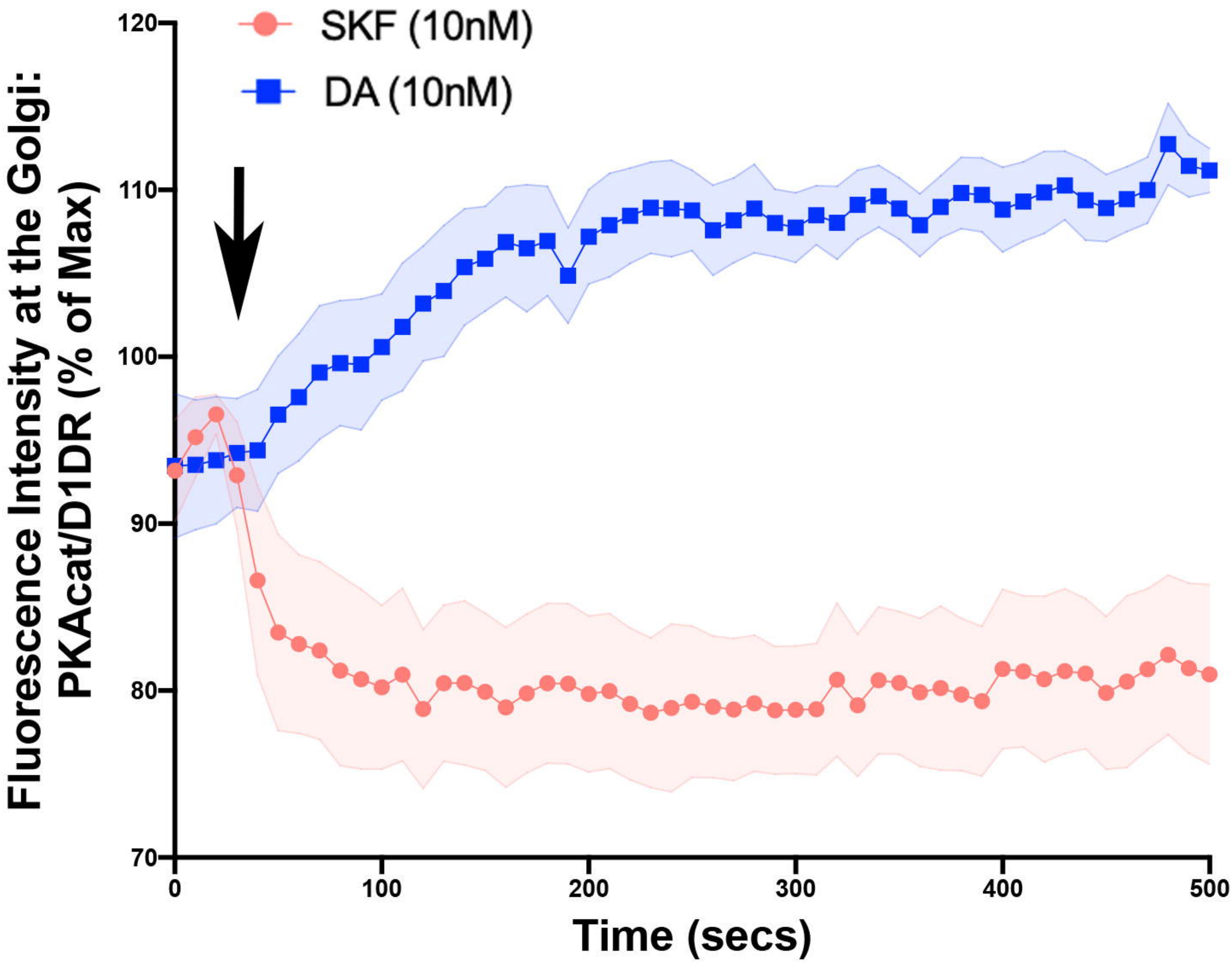
SKF (10nM)
DA (10nM)
Fluorescence Intensity at the Golgi:
PKAcat/D1DR (% of Max)
120
110
100
90
80
70
0
100
200
300
400
500
Time (secs)